Unsupported Standing With Minimized Ankle Muscle Fatigue

Matjaž Mihelj* and Marko Munih, *Member, IEEE*

***Abstract*—In the past, limited unsupported standing has been restored in patients with thoracic spinal cord injury through open-loop functional electrical stimulation of paralyzed knee extensor muscles and the support of intact arm musculature. Here an optimal control system for paralyzed ankle muscles was designed that enables the subject to stand without hand support in a sagittal plane. The paraplegic subject was conceptualized as an underactuated double inverted pendulum structure with an active degree of freedom in the upper trunk and a passive degree of freedom in the paralyzed ankle joints. Control system design is based on the minimization of a cost function that estimates the effort of ankle joint muscles via observation of the ground reaction force position, relative to ankle joint axis. Furthermore, such a control system integrates voluntary upper trunk activity and artificial control of ankle joint muscles, resulting in a robust standing posture. Figures are shown for the initial simulation study, followed by disturbance tests on an intact volunteer and several laboratory trials with a paraplegic person. Benefits of the presented methodology are prolonged standing sessions and in the fact that the subject is able to maintain voluntary control over upper body orientation in space, enabling simple functional standing.**

***Index Terms*—Optimal control, paraplegia, unsupported standing.**

I. Introduction

ARM-SUPPORTED standing and limited crutch- or walker-assisted walking can be restored in patients with spinal cord injuries through functional electrical stimulation or mechanical bracing of paralyzed lower extremities [1]. For these patients, standing has many beneficial effects, both physiological and psychological in nature [2]. Physically, standing may prevent joint contractures by interrupting the chronic sitting posture and may diminish osteoporosis. The upright posture may also improve functioning of the internal organs and aid in bowel and bladder function. In addition, a standing posture may provide a platform for accomplishing everyday activities. For example, a paraplegic patient would be able to reach some objects while standing that could not be reached from the confines of a wheelchair. These increased functional abilities may enhance personal self-esteem while providing a level of independence. Considerable effort is therefore being invested into finding an efficient methodology that would enable a paraplegic person to stand without arm support. An important reason for renewed interest in standing is an appreciation of the central importance of the actions of the neurologically intact neuromuscular system of the upper body. The realization that the number of degrees of freedom (DOFs) of the paraplegic body is such that posture may still be controllable by the intact neuromuscular system suggests that artificial controllers for standing should be designed on this basis [3].

In order to achieve unsupported standing, the body's center of gravity has to be controlled over a relatively small support surface. To achieve this, paralyzed ankle joints inevitably need to be feedback controlled, because during standing they are positioned far from anatomical motion boundaries. In contrast, knee and hip joints affected by paraplegia can simply be stabilized with an open-loop control or mechanical braces in a hyperextended position [4], [5]. Because energy-efficient postures for stable standing are very limited, the selected balance control methodology needs to be efficient and robust.

Unsupported standing has only recently been achieved by bracing the paraplegic person's body above the calves in a single link inverted pendulum structure and applying electrical stimulation to the ankle joint plantarflexors [6], [7]. The paralyzed person does not have any voluntary control over this standing posture, being specified by the ankle joint angle reference. In order to simplify the control strategy and limit muscle activation to the ankle plantarflexor group, an anterior posture is maintained. The methodology allows relatively long standing exercises; however, the unnatural fixation and rapid muscle fatigue severely hinder its utility. Posture control relies on an artificial balancing algorithm alone, and there is no supporting activity from intact musculature.

A control strategy for unsupported paraplegic standing, utilizing the residual sensory and motor abilities of a thoracic spinal cord injured subject, was proposed by Matjačić and Bajd [5], [8] in 1998. The strategy is based on voluntary and reflex activity of the patient's upper body and artificially controlled stiffness in the ankles. The knees and hips are maintained in the extended position by long leg braces or functional electrical stimulation. This way, the subject is constrained in an underactuated double link inverted pendulum structure with one DOF in the paralyzed ankle joints and the other in the lumbosacral joint which is under subject's voluntary control (underactuated indicates a system that has fewer actuators than DOFs; in this case, the only actuator is the upper trunk muscles because there is no actuation in the ankle joints except passive stiffness). In a detailed analysis of this underactuated system, Matjačić

Manuscript received October 16, 2002; revised November 23, 2003. This work was supported by the Ministry of Education, Science, and Sport, Republic of Slovenia. *Asterisk indicates corresponding author.*

*M. Mihelj is with the University of Ljubljana, Faculty of Electrical Engineering, Tržaška 25, SI-1000 Ljubljana, Slovenia (e-mail: matjaz.mihelj@robo.fe.uni-lj.si)

M. Munih is with the University of Ljubljana, Faculty of Electrical Engineering, SI-1000 Ljubljana, Slovenia (e-mail: marko.munih@robo.fe.uni-lj.si).

Digital Object Identifier 10.1109/TBME.2004.827560

and Bajd [8] showed that such unsupported balancing is not feasible unless artificial stiffness is introduced in the paralyzed ankle joints. When assisted by an artificial ankle joint stiffness value of 8Nm/° or more, the paraplegic subject was capable of the proposed balancing. With the upper trunk free to move, the subject retains voluntary control over upright posture, an important step toward functional standing.

Understanding the unimpaired subject's control over constrained balancing provides useful information for further improving the quality of the proposed control strategy. Analysis of unimpaired subject stance indicates a combined ankle–hip strategy as the most used sequence of responses to anterior–posterior disturbances [9]. Leaning of the subject around the ankles prior to the disturbance also affects the overall postural strategy for disturbance rejection [10]. Subjects use a different postural strategy when perturbed while leaning near their forward or backward limits of stability. An important feature of postural dynamics is the effect of the forward lean, which results in a significant increase in the tonic component of ankle torque. Postural stability is improved here by simplifying the response to the perturbation [11], because the risk of falling backward is reduced by increasing the stability margin between the center of gravity and the posterior limits of the base of support. Following that, the postural ankle dynamics can be based on a single muscle group—ankle plantarflexors.

However, a major issue in any application based on functional electrical stimulation is the fatiguing of stimulated muscles. Rapid muscle fatigue during standing can result in loss of balance, leading to new traumas. During stiffness-supported standing, the subject controls muscle fatigue by using the upper trunk for balance, therefore reducing its functionality. In order to reduce the burden of fatigue, an artificial control system needs to be designed in such a way as to allow sustained functionality of the upper trunk and minimize fatiguing by its own rules. The greatest source of ankle muscle fatigue is compensation of the gravity-generated torque around the ankle joints. In order to minimize this torque, the vertical projection of the total body's center of mass needs to be located within close proximity of the ankle joint axis. Another major contribution to muscle fatigue is the control of body sway in an anterior/posterior direction and the associated torque required to sustain vertical body equilibrium.

This paper makes advances on the issues highlighted above. Closed-loop control of ankle plantar and dorsal flexors with voluntary-sway control in the upper trunk is utilized. The algorithms are based on minimal loading of stimulated muscles.

II. Methods

A. Stance Dynamics

To restore functional unsupported standing, a robust control system must be synthesized that can provide support for upright balance and minimize stimulated muscle fatigue, and at the same time allow the user to retain full control over the posture acquired. These are the features required from the control system. Neurologically intact subjects usually base their task executions on minimization of a task-dependent cost function, thus from the control point of view tending toward optimality. Similarly, the artificial posture control methodology requires minimization of ankle muscle effort, and therefore we based the control synthesis on optimal control theory. Its implementation requires selection of optimization criteria comprising all control objectives.

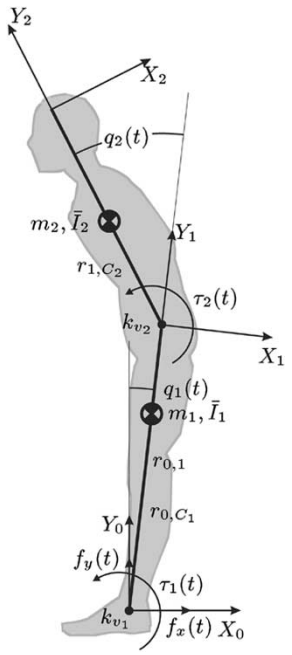

Fig. 1. Double inverted pendulum structure: feet—support surface; lower extremities—first segment; trunk, head, and arms—second segment. Centers of masses of both segments and their distances from joints r_{0,C_1} and r_{1,C_2} are shown. The lower body link length is noted with $r_{0,1}$. $q_1(t)$ and $q_2(t)$ are the ankle and trunk joint angles, respectively; τ_1, τ_2 are the net torques produced by FES of muscles in the ankle joint and by voluntary activation in the trunk. m_1, m_2 are the masses of both links and $\bar{I}_1$, $\bar{I}_2$ are the moments of inertia around the mass centers of each link. k_{v_1} and k_{v_2} are coefficients of viscous friction for ankle and trunk joints, respectively.

The center of pressure (CoP) or the position of ground reaction force relative to the ankle joint axis is the biomechanical variable that complexly denotes ankle muscle effort due to gravity-generated torque and body acceleration when swaying. As such it provides adequate starting point for the optimal control system cost function selection.

Further analysis is based on the assumption that standing posture can be simplified as a double inverted pendulum structure with one DOF in the ankle joint axis and the other in the lumbosacral joint (Fig. 1). Hemami *et al.* [12]–[14] and Matjačić and Bajd [8] developed one- and two-link inverted pendulum models to study feedback control to stabilize posture. The approach from [8] was adopted here, where nonlinear equations of motion were derived by the Newton–Euler method. As the body dynamics during standing have been demonstrated to be fairly linear [8], [13], [15], and since the objective of the paraplegic subject is to maintain an upright posture, we can linearize the double inverted pendulum model around the vertical equilibrium. Assuming quasi-static motion and small angular deviations from the vertical equilibrium, the following simplifications were used: $\dot{q}^2(t) = 0$, $\sin q(t) = q(t)$, and $\cos q(t) = 1$. In concert with the notations in Fig. 1 and with the definitions $r_{0,C_2} = r_{0,1} + r_{1,C_2}$, $I_1 = \bar{I}_1 + r_{0,C_1}^2 m_1$, $I_2 = \bar{I}_2 + r_{1,C_2}^2 m_2$,

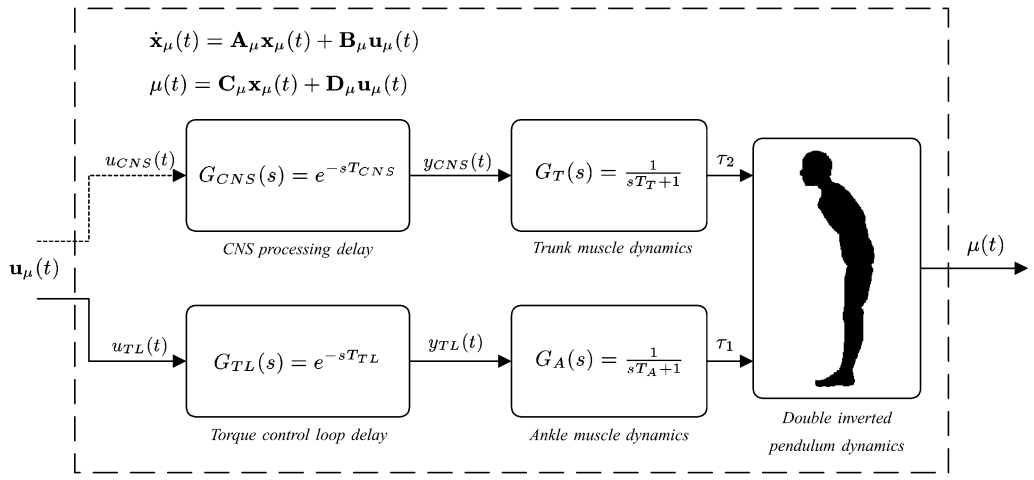

Fig. 2. Open-loop dynamics consists of processing delays, muscle activation dynamics, and double inverted pendulum dynamics.

$I_{02} = \bar{I}_2 + r_{0,C_2}^2 m_2$, and $I_{12} = \bar{I}_2 + r_{0,C_2} r_{1,C_2} m_2$, the linearization of double inverted pendulum inverse dynamics around vertical equilibrium yields the following equations:

$$\begin{aligned}\tau_1(t) =& -g(r_{0,C_1}m_1 + r_{0,C_2}m_2)q_1(t) - gr_{1,C_2}m_2 q_2(t) \\ &+ k_{v_1}\dot{q}_1(t) + (I_1 + I_{02})\ddot{q}_1(t) + I_{12}\ddot{q}_2(t) \quad (1)\\ \tau_2(t) =& -gr_{1,C_2}m_2(q_1(t) + q_2(t)) + k_{v_2}\dot{q}_2(t) \\ &+ I_{12}\ddot{q}_1(t) + I_2\ddot{q}_2(t) \quad (2)\\ f_x(t) =& -(r_{0,C_1}m_1 + r_{0,C_2}m_2)\ddot{q}_1(t) - r_{1,C_2}m_2\ddot{q}_2(t) \quad (3)\\ f_y(t) =& g(m_1 + m_2). \quad (4)\end{aligned}$$

Equations (1) and (2) determine ankle and trunk torque, respectively. Equations (3) and (4) determine two components of the force acting in the ankle joint. A linear direct dynamics model can be obtained by expressing joint variables as a function of joint torques

$$\begin{aligned}\dot{\mathbf{q}}(t) &= \mathrm{A}_P\mathbf{q}(t) + \mathrm{B}_P\boldsymbol{\tau}(t)\\ \mathbf{q}(t) &= \mathrm{C}_P\mathbf{q}(t) + \mathrm{D}_P\boldsymbol{\tau}(t) \quad (5)\end{aligned}$$

where $\mathbf{q}(t) = [q_1(t) \quad \dot{q}_1(t) \quad q_2(t) \quad \dot{q}_2(t)]^T$ and $\boldsymbol{\tau}(t) = [\tau_1(t) \quad \tau_2(t)]^T$ (see Appendix I for details).

These equations describe only the body dynamics. In order to obtain a robust posture control system, delays deriving from information processing and command issuing are also further considered, as well as activation dynamics inherent to different muscle groups. Fig. 2 depicts a schematic view of unsupported standing dynamics, consisting of body (pendulum) dynamics, actuating muscles, and inherent local control loops, either natural or artificial. Each joint of the double inverted pendulum structure, including trunk and ankle, is activated by a set of muscles divided into agonist and antagonist groups. The intact upper trunk muscle groups are functionally linked to the central nervous system (CNS) and as such are under the subject's voluntary control. The processing delay inherent to the CNS was considered as a pure time delay with the transfer function

$$G_{\mathrm{CNS}}(s) = e^{-sT_{\mathrm{CNS}}} \quad (6)$$

where T_{CNS} represents an empirical time delay constant. The ankle muscle groups affected by paraplegia have no immediate connection to the CNS; thus an artificial ankle joint torque control system was designed based on variable structure system theory [16]. The dynamics have been simplified with the transfer function

$$G_{\mathrm{TL}}(s) = e^{-sT_{\mathrm{TL}}} \quad (7)$$

where T_{TL} indicates pure time delay. Signals from either the CNS or torque controller define muscle activation. Muscle activation dynamics were approximated with first-order transfer functions. Activation dynamics of trunk extensor and flexor muscles were modeled as

$$G_T(s) = \frac{1}{sT_T + 1} \quad (8)$$

where T_T is an empirically determined time constant. Similarly, activation dynamics of ankle plantarflexor and dorsiflexor muscle groups were approximated with the transfer function

$$G_A(s) = \frac{1}{sT_A + 1} \quad (9)$$

where T_A is again an empirically determined time constant.

Taking into consideration the linearized double inverted pendulum dynamics (5), processing delays (6) and (7), and muscle activation dynamics (8) and (9), the plant dynamics can be rewritten in a state space form as

$$\begin{aligned}\dot{\mathbf{x}}_\mu(t) &= \mathrm{A}_\mu\mathbf{x}_\mu(t) + \mathrm{B}_\mu\mathbf{u}_\mu(t)\\ \boldsymbol{\mu}(t) &= \mathrm{C}_\mu\mathbf{x}_\mu(t) + \mathrm{D}_\mu\mathbf{u}_\mu(t). \quad (10)\end{aligned}$$

The expression $\mathbf{x}_\mu(t)$ [(II.5); see Appendix II] indicates the plant state vector that combines states of all subsystems, namely, torque control loop dynamics, CNS processing delay, activation dynamics of ankle and trunk muscles, and angles and angular velocities of double inverted pendulum structure. The plant input vector $\mathbf{u}_\mu(t)$ [(II.6)] consists of ankle and trunk torque reference signals, and the plant output vector $\boldsymbol{\mu}(t)$ [(II.7)] includes all directly measured system variables, namely, ankle torque as well as angles and angular velocities of double inverted pendulum structure.

With the standing dynamics completed, the description will now focus on kinematic and dynamic relations in the foot during standing (Fig. 3). Since we are concerned with stable posture, we employ additional constraints involved with maintaining stability—keeping the feet flat on the ground. We assume that either the toes or heels off the ground is a prelude to a less stable

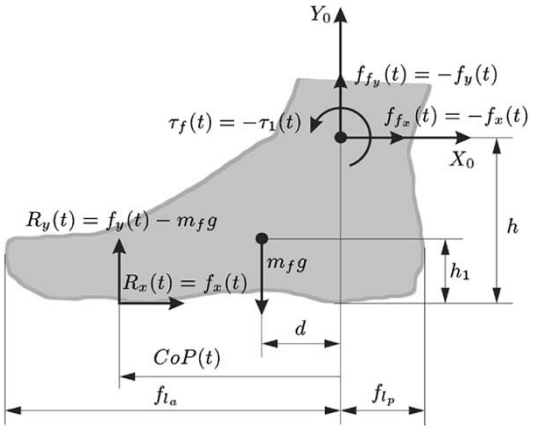

Fig. 3. Kinematic and dynamic relations in foot during standing—estimation of ground reaction force position CoP(t) resulting from forces and torque acting on the foot expressed in the base coordinate system (X_0, Y_0) located in the ankle joint. Force $f_f(t)$ and torque $\tau_f(t)$ are exerted on the foot by a lower body link and R is the ground reaction force. Force $f(t) = -f_f(t)$ and torque $\tau_1(t) = -\tau_f(t)$ are exerted on the lower body link by the foot. The height of the ankle joint is noted with h; h_1 is the height of the center of gravity of the foot; d is the horizontal distance between the ankle joint and the center of gravity of the foot; and m_f is the mass of the foot.

configuration [17]. Because in this case foot linear and angular acceleration equals zero during quiet standing, the position of CoP(t) can be determined only as a function of forces and torque acting in the ankle joint. Force and torque equilibrium equations for the foot can be written based on the relations in Fig. 3 as

$$R_x(t) + f_{f_x}(t) = 0 \Longrightarrow R_x(t) = f_x(t) \tag{11}$$

$$R_y(t) + f_{f_y}(t) + m_f g = 0 \Longrightarrow R_y(t) = f_y(t) - m_f g \tag{12}$$

and

$$\tau_f(t) = f_{f_x}(t)(h - h_1) - f_{f_y}(t)d - R_x(t)h_1 + R_y(t)(-\mathrm{CoP}(t) - d). \tag{13}$$

Combination of (11)–(13) gives the ground reaction force position CoP(t), expressed in the base coordinate frame (X_0, Y_0)

$$\mathrm{CoP}(t) = -d - \frac{-\tau_1(t) - d f_y(t) + h f_x(t)}{f_y(t) - m_f g}$$

$$\xrightarrow{m_f \ll m_1 + m_2} \mathrm{CoP}(t) = \frac{\tau_1(t) - h f_x(t)}{f_y(t)}. \tag{14}$$

In (14) we assumed $m_f \ll m_1 + m_2$ and therefore neglected the term $m_f g$. The following inequality, which poses a constraint on the dynamics of the mechanical model, must be satisfied [8]:

$$-f_{l_a} < \mathrm{CoP}(t) < f_{l_p}. \tag{15}$$

It should be noted that the lengths f_{l_a} and f_{l_p} place biomechanical constraints on the plantarflexor and dorsiflexor torques that can act around the ankle joint, without lifting the heels or toes. On the other hand, the subject's total mass, and the frictional properties of the contact with the floor, determine the upper bound on the magnitude of the shear force at the ground, which in turn determines the upper bound on the torque $\tau_2(t)$ [8]. With the combination of (1), (3), and (4) into (14), and considering the direct dynamics model (5), the CoP(t) can be described as a function of the state vector $\mathbf{q}(t)$ and the joint torque vector $\boldsymbol{\tau}(t)$ as

$$\mathrm{CoP}(t) = (\mathbf{U}^T + \mathbf{V}^T \mathrm{A}_P)\mathbf{q}(t) + \mathbf{V}^T \mathrm{B}_P \boldsymbol{\tau}(t) \tag{16}$$

where

$$\mathbf{U} = \frac{1}{g(m_1 + m_2)} \begin{bmatrix} -g(r_{0,C_1} m_1 + r_{0,C_2} m_2) \\ k_{v_1} \\ -g r_{1,C_2} m_2 \\ 0 \end{bmatrix}$$

and

$$\mathbf{V} = \frac{1}{g(m_1 + m_2)} \begin{bmatrix} 0 \\ I_1 + I_{02} + h(r_{0,C_1} m_1 + r_{0,C_2} m_2) \\ 0 \\ I_2 + r_{1,C_2}(h + r_{0,1}) m_2 \end{bmatrix}.$$

Further, considering the plant state space model (10) and the relationship between the double inverted pendulum state space vector $\mathbf{q}(t)$ and the plant state space vector $\mathbf{x}_\mu(t)$, the position CoP(t) can be rewritten as a function of system states $\mathbf{x}_\mu(t)$ and inputs $\mathbf{u}_\mu(t)$ as

$$\mathrm{CoP}(t) = \left(\mathbf{U}_\mu^T + \mathbf{V}_\mu^T \mathrm{A}_\mu\right) \mathbf{x}_\mu(t) + \mathbf{V}_\mu^T \mathrm{B}_\mu \mathbf{u}_\mu(t) \tag{17}$$

where $\mathbf{U}_\mu$ and $\mathbf{V}_\mu$ vectors were introduced as

$$\mathbf{U}_\mu^T = [\,\mathbf{0}^{1\times 10} \quad \mathbf{U}^T\,]$$
$$\mathbf{V}_\mu^T = [\,\mathbf{0}^{1\times 10} \quad \mathbf{V}^T\,]. \tag{18}$$

B. Control Algorithm

Because the body dynamics have been demonstrated to be fairly linear and the closed-loop system composed of both the CNS and the body dynamics appears to be linear [4], the CNS can be expected to behave linearly as well. It is assumed that the CNS, though composed of many nonlinear neural elements, will behave linearly about the operating point corresponding to upright standing [15]. Such behavior of the CNS allows us to base the design of the controller for unsupported standing on linear control theory.

Based on the redefined CoP(t) position (17), a cost function for an optimal control system design was selected as

$$J(\mathbf{x}_\mu(t), \mathbf{u}_\mu(t)) = \int_0^\infty \left(\mathrm{CoP}^T(t)\mathrm{CoP}(t) + \mathbf{u}_\mu^T(t)\mathrm{R}\mathbf{u}_\mu(t)\right) dt$$
$$= \int_0^\infty \Big(\mathbf{x}_\mu^T(t)\mathrm{R}_{\mathbf{xx}}\mathbf{x}_\mu(t) + 2\mathbf{x}_\mu^T(t)\mathrm{R}_{\mathbf{xu}}\mathbf{u}_\mu(t) + \mathbf{u}_\mu^T(t)\mathrm{R}_{\mathbf{uu}}\mathbf{u}_\mu(t)\Big) dt. \tag{19}$$

The cost function is selected in a way to penalize large deviations of CoP(t) from the ankle joint axis resulting in minimal effort required for unsupported standing. The term $\mathbf{u}_\mu^T(t)\mathrm{R}\mathbf{u}_\mu(t)$ represents a penalty that helps the designer on one hand keep the magnitude of $\mathbf{u}_\mu(t)$ small and on the other hand determine the relative importance of elements of vector $\mathbf{u}_\mu(t)$. Hence the control weighting matrix R influences how small components of $\mathbf{u}_\mu(t)$ will be. For simplicity an identity matrix was used for R in our case. Finally, the cost function relates the cost value to the plant states through the weight matrix $\mathrm{R}_{\mathbf{xx}}$, to the plant inputs through the weight matrix $\mathrm{R}_{\mathbf{uu}}$, and to states and inputs through the cross-weighting matrix $\mathrm{R}_{\mathbf{xu}}$ (see Appendix III for

details on weighting matrices). All matrices are directly determined from the subjects' anthropometric data.

If the following assumptions hold [18]:

1) the entire state vector $\mathbf{x}_\mu(t)$ is available for feedback;
2) $\mathrm{R}_{\mathbf{xx}} = \mathrm{R}_{\mathbf{xx}}^T \geq 0$, $\mathrm{R}_{\mathbf{uu}} = \mathrm{R}_{\mathbf{uu}}^T > 0$, and $\begin{bmatrix} \mathrm{R}_{\mathbf{xx}} & \mathrm{R}_{\mathbf{xu}} \\ \mathrm{R}_{\mathbf{xu}}^T & \mathrm{R}_{\mathbf{uu}} \end{bmatrix} \geq 0$;
3) $\begin{bmatrix} \mathrm{A}_\mu & \mathrm{B}_\mu \end{bmatrix}$ is stabilizable (a system is stabilizable if all its uncontrollable modes decay to zero asymptotically) and $\begin{bmatrix} \mathrm{A}_\mu & \mathrm{R}_{\mathbf{xx}}^{1/2} \end{bmatrix}$ is detectable (a system is detectable if all its unobservable modes decay to zero asymptotically);

then

1) the linear quadratic controller is unique, optimal full-state feedback control law

$$\mathbf{u}_\mu(t) = -{}^{LQ}K\mathbf{x}_\mu(t) \text{ with } {}^{LQ}K = \mathrm{R}_{\mathbf{uu}}^{-1}\left(\mathrm{R}_{\mathbf{xu}}^T + \mathrm{B}_\mu^T\mathrm{S}\right) \quad (20)$$

that minimizes the cost $J(\mathbf{x}_\mu(t), \mathbf{u}_\mu(t))$, subject to the dynamic constraints in (10);

2) by defining $\mathrm{A}_r = \left(\mathrm{A}_\mu - \mathrm{B}_\mu\mathrm{R}_{\mathbf{uu}}^{-1}\mathrm{R}_{\mathbf{xu}}^T\right)$, S is the unique, symmetric, positive semidefinite solution to the algebraic Riccati equation

$$\mathrm{SA}_r + \mathrm{A}_r^T\mathrm{S} + \left(\mathrm{R}_{\mathbf{xx}} - \mathrm{R}_{\mathbf{xu}}\mathrm{R}_{\mathbf{uu}}^{-1}\mathrm{R}_{\mathbf{xu}}^T\right) - \mathrm{SB}_\mu\mathrm{R}_{\mathbf{uu}}^{-1}\mathrm{B}_\mu^T\mathrm{S} = 0 \quad (21)$$

3) the closed-loop dynamics derived by substitution of (20) into (10) are guaranteed to be asymptotically stable [18].

Because only the system states pertaining to the output vector can directly be measured, a Kalman full state observer was designed to estimate the full state vector $\hat{\mathbf{x}}_\mu(t)$ as

$$\dot{\hat{\mathbf{x}}}_\mu(t) = \mathrm{F}_K\hat{\mathbf{x}}_\mu(t) + \mathrm{B}_\mu\mathbf{u}_\mu(t) + \mathrm{G}_K\boldsymbol{\mu}(t) \quad (22)$$

where $\mathrm{F}_K = \mathrm{A}_\mu - \mathrm{G}_K\mathrm{C}_\mu$ [19]. Equation (22) has a form of Luenberger observer, with Kalman gain matrix G_K defined as

$$\mathrm{G}_K = \Sigma\mathrm{C}_\mu^T\mathrm{S}_{\mathbf{v}}^{-1}. \quad (23)$$

The $\mathrm{S}_{\mathbf{v}}$ is symmetric and positive definite sensor noise intensity matrix and Σ denotes unique, symmetric, and at least positive semidefinite, $\Sigma = \Sigma^T \geq 0$, solution matrix of the filter algebraic Riccati equation

$$\mathrm{A}_\mu\Sigma + \Sigma\mathrm{A}_\mu^T + \mathrm{B}_{\boldsymbol{\mu}}\mathrm{S}_{\mathbf{w}}\mathrm{B}_{\boldsymbol{\mu}}^T - \Sigma\mathrm{C}_\mu^T\mathrm{S}_{\mathbf{v}}^{-1}\mathrm{C}_\mu\Sigma = 0 \quad (24)$$

with $\mathrm{S}_{\mathbf{w}}$ symmetric and positive definite process noise intensity matrix.

With the control designed as in (20), the controller would tend to minimize the ankle torque, therefore bringing it close to zero. However, due to the forward/backward asymmetric support surface, it is not desirable to set the position of the vertical projection of the body center of mass in proximity to the ankle joint axis, because stability margins for posterior disturbances would narrow. Experiments performed on intact subjects indicate that a slightly anterior posture produces much more robust standing in respect to disturbance activity. From there, it is preferable to maintain a slightly anterior posture by adding offset value to the ankle torque operating point for the posture control system. With the new vector $\boldsymbol{\tau}_0(t)$ that determines desired torque operating point, the control algorithm can be finally modified as

$$\mathbf{u}_\mu(t) = -{}^{LQ}\mathrm{K}\left(\hat{\mathbf{x}}_\mu(t) - \hat{\mathbf{x}}_{\mu,0}(t)\right) + \boldsymbol{\tau}_0(t). \quad (25)$$

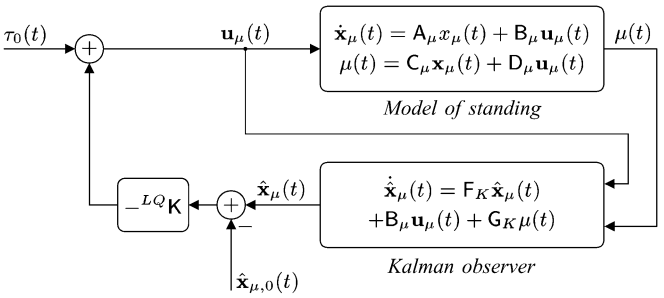

Fig. 4. Selection of ankle torque operating point $\boldsymbol{\tau}_0(t)$.

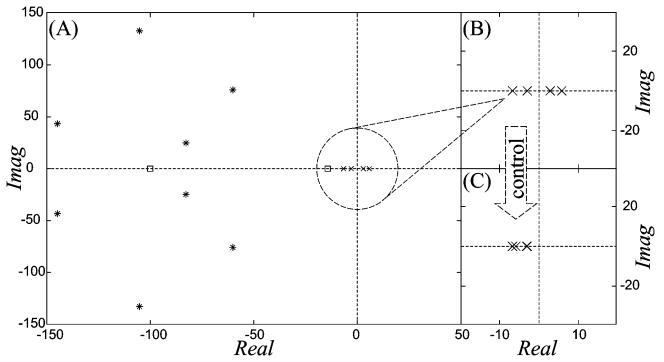

Fig. 5. (a) Open-loop linearized system poles: double inverted pendulum ($\times$), muscle dynamics ($\square$), processing delays ($*$); (b) close examination of double inverted pendulum poles; (c) double inverted pendulum poles after controller implementation.

The $\hat{\mathbf{x}}_{\mu,0}(t)$ defines adequate systems states at the operating point $\boldsymbol{\tau}_0(t)$ as

$$\hat{\mathbf{x}}_{\mu,0}(t) = -\mathrm{F}_K^{-1}\left(\mathrm{I} - \mathrm{G}_K\mathrm{C}_\mu\mathrm{A}_\mu^{-1}\right)\mathrm{B}_\mu\boldsymbol{\tau}_0(t). \quad (26)$$

The block diagram of the plant and the control system are presented in Fig. 4 with the feedback just designed presenting the posture control loop. The input to the system $\boldsymbol{\mu}(t)$ is measured segment positions, velocities, and ankle torque. The output of the posture control system is passed as a torque reference to the torque control loop not presented here [16]. An optimal control design approach enables attainment of unsupported standing without explicitly prescribing the desired posture, and at the same time maintains reduced ankle muscle fatigue. The user is free to select the orientation of the upper body in space as a voluntary action, because upright balance is then automatically maintained by rotation of the ankle joints to the angle at which ankle torque coincides with the prescribed torque operating point.

The unsupported standing dynamics (10) is an inherently unstable system. For a subject with a mass of 64 kg, a height of 1.74 m, an ankle/hip distance of 0.81 m, a hip/shoulder distance of 0.59 m, processing delays equal to 0.1 s, and a muscle dynamics time constant of 0.1 s, the linearized system poles are shown in Fig. 5(a). The poles pertaining to the Pade functions and muscle activation dynamics are all stable and mostly far on the left half-plane. However, two of the double inverted pendulum poles are located in the right half-plane [see Fig. 5(b) for details], thus resulting in an unstable system. The artificially designed optimal control system stabilizes the double inverted pendulum. Poles of the combined plant-controller system are

Fig. 6. Experimental setup.

located in the left half-plane as presented in Fig. 5(c). The designed control system shifts only poles of the double inverted pendulum structure, while the poles pertaining to the activation dynamics and signal processing remain unchanged.

C. Experimental Setup

Fig. 6 shows the experimental setup with an intact subject placed in the mechanical rotating frame (MRF). The device constrains the body by allowing movements only in the upper trunk and ankle joints, while the arms are folded on the chest. The device consists of a base fixation, a rotating frame, and a hydraulic actuating system. The rotating part of the device consists of a frame that provides bracing to the lower body and forces the knees and hips into an extended position with aluminum bars. The hydraulic actuator mounted in the ankle rotation axis provides the torque required to support standing or produce various disturbances. More details on the MRF are given in [5] and [20]. Two force plates (AMTI, Advanced Mechanical Technology, Inc.) are mounted in the base of the device in order to allow measurement of reaction forces and torques separately for each foot. The movement kinematics were assessed by the optical position measuring system OPTOTRAK (Northern Digital, Inc.) with infrared markers placed on the rotating frame and on the subject's trunk. The joint angles were defined as in Fig. 1. Positive ankle angles correspond to ankle dorsiflexion and positive trunk angles to trunk flexion.

III. Results

Initial evaluation of the posture control system was performed in a simulation-based study, followed by neurologically intact subjects and, finally, a paraplegic patient.

A. Simulation Results

The simulation-based study provides good insight into the control strategy background. In this case a local proportional-derivative controller was used to simulate the CNS task of controlling upper body movement according to a randomly generated trajectory (Fig. 7). Based on random trunk movement and an ankle torque operating point set to -10 Nm, the posture control system generates an ankle torque reference that maintains the double inverted pendulum balanced. The simulation results are presented in Fig. 8. The ankle and trunk angle time courses indicate opposite motion in the trunk and ankle joints. Such trajectories enable a constant body center of mass position, resulting in a constant ankle joint torque close to the prescribed operating point. However, because ankle joint torque presents a control variable, the prescribed operating point value can never be perfectly matched. Small ankle torque changes are necessary to maintain the controlled structure balanced.

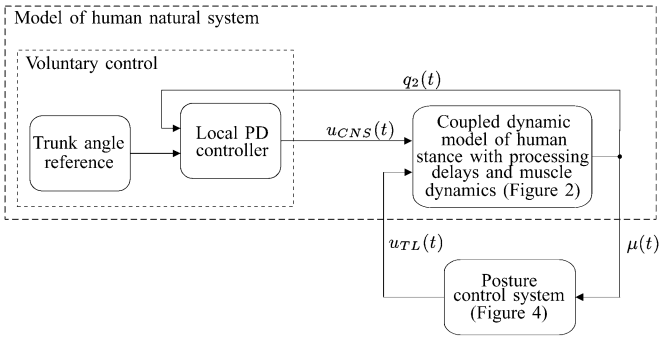

Fig. 7. Simulation of unsupported standing with the implementation of the optimal posture control system.

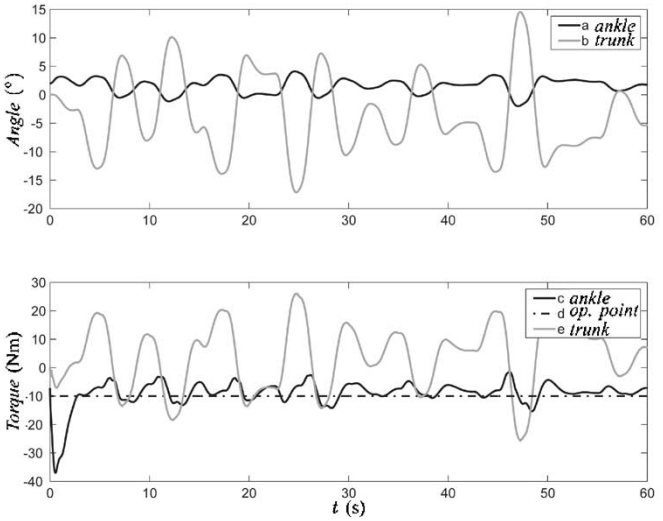

Fig. 8. Unsupported standing simulation; torque operating point -10 Nm.

B. Intact Subject Perturbed Standing

Next we compared the selected control methodology to an intact subject's perturbed stance. The person was constrained as shown in Fig. 6 with the standing perturbed by random disturbances in anterior/posterior direction. The subject was instructed to respond with voluntary and reflex activity based on the perception of the disturbances. In this, the control system had no direct information about the perturbation. The control output was generated in real time based on information registered in the system output vector $\boldsymbol{\mu}(t)$. A detailed comparison of the control system output and subject-generated ankle torque is presented in Fig. 9. A noticeable similarity can be observed in the amplitude of the responses of the intact subject and the posture control system. However, there is a significant difference

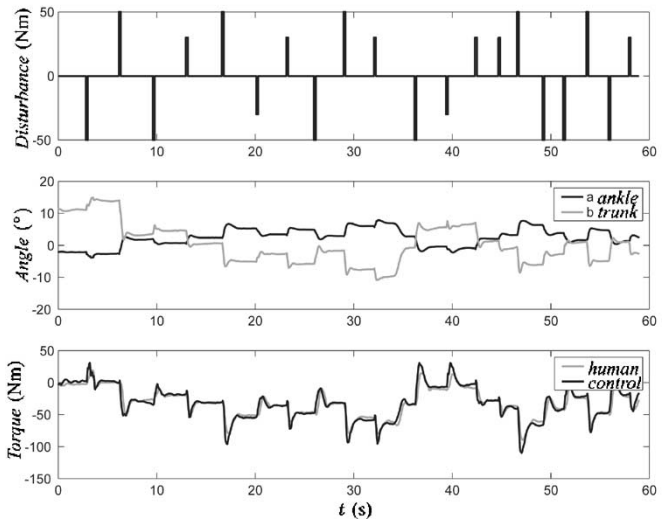

Fig. 9. Comparison between intact subject and artificial controller.

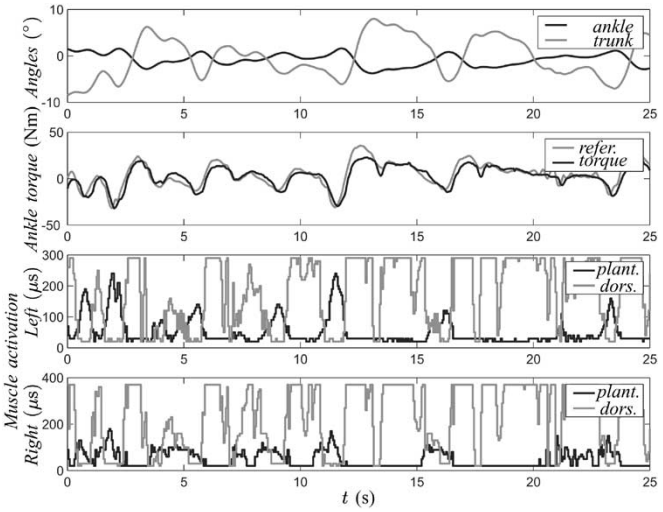

Fig. 11. Paraplegic arm-free standing with voluntary trunk motion.

Fig. 10. Paraplegic subject during unsupported standing.

in the timing of the responses. The cross-correlation analysis indicates that the artificial control system response precedes the subject-generated torque by 100 ms (the measured latency of the subject-generated torque indicates a stretch reflex response [21]). The time difference is small but extremely important, because the delays of the torque control loop summarize to approximately the same value. From there, the response time of the artificial control system including posture control loop and ankle torque control loop would be equal to the response time of a neurologically intact subject.

C. Paraplegic Standing

Finally, the efficiency of the control system designed was evaluated on a paraplegic patient (Fig. 10). The experimental procedure was approved by the national medical ethics committee, and the subject gave informed consent for participation in the study. He was nine months post injury resulting in a complete T6 lesion. Before participating in the research, his ankle muscles underwent a one-month training process. Experiments were performed in two sessions lasting approximately two hours each. Since the injury the subject had no experience with arm-free standing and no preparatory training was conducted during the study. Four channels of 20 Hz frequency surface electrical stimulation were applied on left/right ankle dorsiflexor and plantarflexor muscle groups. The 50-mm-diameter electrodes were placed on the midlines of the soleus and gastrocnemius muscles for the plantarflexor stimulation and on the tibialis anterior muscles for the dorsiflexor stimulation. The stimulation pulse width was varied according to the posture control system output and torque control system algorithm [16].

Results for three distinct standing periods will be analyzed. The first experiment was a repetition of the simulation-based study in real circumstances. The subject was instructed to move his upper trunk freely as presented in Fig. 11. The control system maintained a stable posture with the least ankle joint effort. The time courses of ankle and trunk angles indicate opposite motion, thus enabling low ankle joint torque by maintaining the body center of gravity above the ankle joint axis. The overall posture was stable and the average measured torque close to the prescribed operating point of -10 Nm. Even though the subject had no difficulties with balancing for the length of the trial, such a posture could probably not be maintained for an extended period of time due to the prevailing stimulation of the dorsiflexor muscle group constituting the weaker muscles of the ankle joints. The reason for the prevailing activation of dorsiflexor muscles is the slightly posterior posture that the subject usually adopted in this case. Even though a maximal stimulation of the dorsiflexors was applied, this was not sufficient to result in an anterior posture. Active trunk movement acting on the ankle joints through dynamic coupling would be required to switch the posture; however, due to the lack of training already mentioned, the subject was unable to perform this.

For the second experiment the torque operating point was set to -40 Nm, leading to an anterior standing posture that required sustained plantarflexor muscle effort (Fig. 12). Despite the fact that ankle torque remains constant throughout the session, it is obvious that the stimulation level of plantarflexor muscles monotonically increases, indicating rapid muscle fatiguing. After only 80 s of such standing, the stimulation level reaches

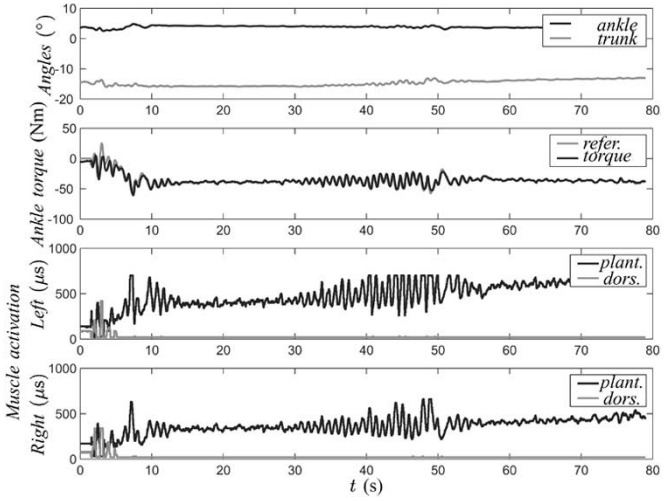

Fig. 12. Paraplegic standing—increased fatigue.

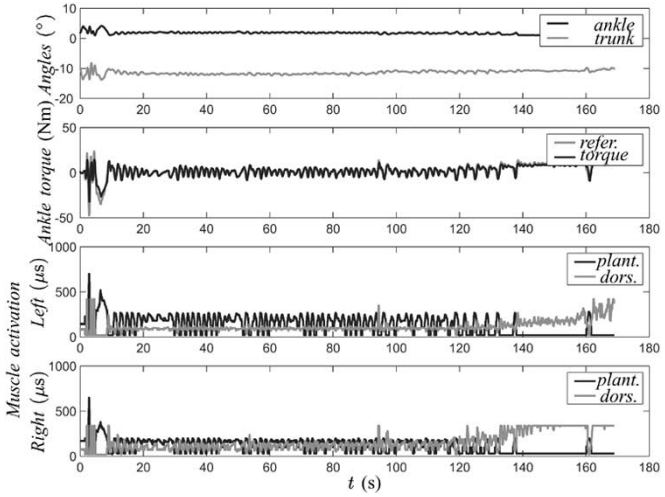

Fig. 13. Paraplegic standing—minimum effort.

saturation value. Due to the fatigued muscles, the subject is no longer able to sustain an upright posture and falls in an anterior direction (safety was provided with a climbing belt and ropes attached to the ceiling). A detailed analysis of muscle properties indicates a 50% decrease of muscle gain in the last 60 s.

The results of the third trial in Fig. 13 indicate prolonged unsupported standing that can be achieved by defining an ankle torque operating point close to zero. The stimulation pattern indicates coactivation of dorsiflexor and plantarflexor muscle groups due to a very low ankle torque. No significant fatiguing occurred in a 3-min-long trial that finished when the person acquired a far posterior posture, and thus overloaded the dorsiflexor muscle group. Being unable to generate active trunk movement at some point to switch to anterior posture, the subject fell backward.

IV. Discussion

The assumption and maintenance of upright posture is such a common occurrence among human beings that it is perhaps the most universally accepted measure of normality [22]. In complete paraplegic subjects, the functional benefit of standing may be larger than that of a gait. While standing provides an important platform for accomplishing everyday activities, traveling over more than short distances will still be much easier in a wheelchair.

This paper reports on a method to synthesize the artificial control of unsupported standing in paraplegia, based on artificial control of paralyzed ankle muscles and the voluntary activity of upper body musculature. The controller designed is subordinated to the subject's voluntary activity and thus enables the user to maintain control of upper body orientation in space. The decision on ankle electrical stimulation activity is based on implicit detection of subject volition through observation of the subject's upper body activity.

The control methodology is based on previous analytical and empirical results that indicate ground reaction force position as an ideal criterion for energy efficiency and stability of unsupported standing. The control criterion includes minimization of stimulated ankle muscle effort, with the purpose of prolonging unsupported standing time. Simplified control rules are as follows. Voluntary upper body anterior motion leads to an anterior position of ground reaction force relative to ankle joint axis requiring higher ankle muscle effort. In order to minimize the effort, the control system increases the activation of plantarflexor muscles, as a consequence moving the entire body posterior and ground reaction force toward the ankle joint axis. Because only a small change in ankle joint angle is necessary to compensate for upper trunk motion, the lower body correction does not considerably influence the upper body orientation in space. In this way the subject efficiently maintains control over upper body orientation in space with the least ankle joint effort. In contrast, in the case of a single inverted pendulum [6], [7], the subject is not allowed to move the upper body, and therefore ankle muscle effort is determined by the ankle joint angle. In the case of stiffness-supported double inverted pendulum standing [5], [8], the rotation of the upper body is followed by rotation of the lower body in the same direction until stiffness-generated torque compensates for gravity-generated torque in ankle joints, all of which leads to increased muscle effort.

The designed control algorithm is based on the force control approach with a specified torque operating point to determine the amount of loading of ankle muscles. An alternative would be an equilibrium point type control with a position setpoint and an impedance field. Such approach with a zero-order impedance controller for paralyzed ankle joints was already successfully implemented [5]. Authors agree that a simple stiffness controller cannot stabilize double inverted pendulum structure. However, a certain ankle stiffness makes standing easier while the task of stabilizing is left to the paralyzed subject, utilizing his residual motor-sensory abilities. Jaime *et al.* [23] proposed the use of a first-order impedance by adding viscosity to pure stiffness for achieving further stabilizing effect. The impedance-type approach is rather attractive since there is no need for a model of the biomechanical structure, which considerably simplifies the design process. On the other hand, the required specification of the position operating point disables the subject from maintaining full control over the standing posture.

Analysis of experimental results of unsupported standing of a paraplegic subject indicates a successful integration of natural and artificial control. The robustness of the standing posture was achieved by decomposing the artificial controller into

two nested loops, with the fast inner control loop presenting the ankle torque control system and the slower outer loop the postural control system shown in this paper. Without any prior experience of arm-free standing supported by functional electrical stimulation, the person was able to maintain vertical balance for prolonged periods of time. Matjačić and Bajd [5], [8] showed that upper body motion assists in maintaining the balance through dynamic coupling, and we therefore believe prolonged training exercise would result in even longer standing sessions. Active upper body dynamics were found important in instances when full ankle joint dorsiflexor muscle stimulation was not sufficient to switch the posture.

The synthesis and analysis of unsupported standing presented has been limited to the sagittal plane only. The subject's body was physically constrained in a double inverted pendulum structure with knees and hips maintained in extension by mechanical braces. The simplification was legitimate, if we consider that these joints do not have a significant impact on the quality of standing. On the other hand, in order to achieve autonomous standing, posture control for the frontal plane also needs to be implemented. Postural responses of healthy subjects to perturbations in multiple directions indicate decoupled control in the sagittal and frontal planes [24]. Based on this assumption, the control of movement in each plane can be designed separately, resulting in a simplified design process. We presume that optimal control strategy would also be satisfactory in the frontal plane; however, the reduced upper body motion space in the frontal plane would require much more hip effort for maintenance of equilibrium. If only the frontal plane control is considered, then the left and right foot are not equally loaded and consequently sagittal plane control also needs to be redistributed between ankle joints in adequate proportions.

This work has not aimed to synthesize fully functional standing due to technical barriers; moreover, limited knowledge of physiological mechanisms does not allow this. Nonetheless, we have demonstrated that an adequate integration of preserved natural sensors and voluntary control with artificially implemented control algorithms for ankle muscle stimulation enables arm-free standing in the sagittal plane. With the subordination of the artificial controller to the subject's voluntary activity, the user is allowed to maintain control over standing posture.

Though the results of the study are encouraging, real functional standing is at this point still not available to the user. In addition to sophisticated control algorithms and selective stimulation methods, adequate sensor systems with high precision need to be designed. Ultimately, artificial sensory feedback from paralyzed extremities also needs to be displayed in an appropriate manner [25] to allow efficient voluntary control over the posture attained.

V. Conclusions

This paper covers the development of a new control strategy for closed-loop control for the restoration of unsupported standing in subjects with spinal cord injuries. The algorithm presented integrates the preserved upper body motor and sensor functions with the artificial control of the paralyzed ankle joints and ensures stable standing of the paraplegic subject constrained in the mechanical rotating frame device limiting motion to the sagittal plane [5]. The control system implicitly detects the subject's volition through the observation of the subject's upper body voluntary action and, based on the optimization criterion, determines an adequate lower body orientation. The proposed control and utilized instrumentation does not allow autonomous standing of a paraplegic person; however, it enables a stable posture in the sagittal plane.

Appendix I
Double Inverted Pendulum Inverse Dynamics Model

The stance inverse dynamics model (5) matrices were defined as

$$\mathrm{A}_P = \begin{bmatrix} 0 & 1 & 0 & 0 \\ \frac{a_{21}}{\Delta} & \frac{k_{v_1} I_2}{\Delta} & \frac{g r_{0,1} r_{1,C_2}^2 m_2^2}{\Delta} & \frac{-k_{v_2} I_{12}}{\Delta} \\ 0 & 0 & 0 & 1 \\ \frac{a_{41}}{\Delta} & \frac{-k_{v_1} I_{12}}{\Delta} & \frac{a_{43}}{\Delta} & \frac{k_{v_2}(I_1+I_{02})}{\Delta} \end{bmatrix} \quad \text{(I.1)}$$

$$\mathrm{B}_P = \begin{bmatrix} 0 & 0 \\ \frac{-I_2}{\Delta} & \frac{I_{12}}{\Delta} \\ 0 & 0 \\ \frac{I_{12}}{\Delta} & \frac{-I_1-I_{02}}{\Delta} \end{bmatrix} \quad \text{(I.2)}$$

where

$a_{21} = -g(I_2 r_{0,C_1} m_1 + \bar{I}_2 r_{0,1} m_2)$;
$a_{41} = -g\left((I_1 + I_{02}) r_{1,C_2} m_2 - I_2(r_{0,C_1} m_1 + r_{0,C_2} m_2)\right)$;
$a_{43} = -g r_{1,C_2} m_2 (I_1 + r_{0,1} r_{0,C_2} m_2)$;
$\Delta = -I_1 I_2 - \bar{I}_2 r_{0,1}^2 m_2$.

Matrix C_P equals identity matrix $\mathrm{I}^{4\times 4}$ and D_P equals zero matrix $0^{4\times 2}$.

Appendix II
Open-Loop Stance Dynamics

Transfer functions $G_{\mathrm{CNS}}(s) = e^{-sT_{\mathrm{CNS}}}$ and $G_{\mathrm{TL}}(s) = e^{-sT_{\mathrm{TL}}}$ were approximated with the fourth-order Pade functions [26]

$$\begin{aligned} G_S(s) &= e^{-sT_S} \\ &\approx \frac{(sT_S)^4 - 20(sT_S)^3 + 180(sT_S)^2 - 840sT_S + 1680}{(sT_S)^4 + 20(sT_S)^3 + 180(sT_S)^2 + 840sT_S + 1680} \end{aligned} \quad \text{(II.1)}$$

and rewritten in matrix form as

$$\begin{aligned} \dot{\mathbf{x}}_S(t) &= \begin{bmatrix} 0 & 1 & 0 & 0 \\ 0 & 0 & 1 & 0 \\ 0 & 0 & 0 & 1 \\ -\frac{1680}{T_S^4} & -\frac{840}{T_S^3} & -\frac{180}{T_S^2} & -\frac{20}{T_S} \end{bmatrix} \mathbf{x}_S(t) + \begin{bmatrix} 0 \\ 0 \\ 0 \\ 1 \end{bmatrix} u_S(t) \\ &= \mathrm{A}_S \mathbf{x}_S(t) + \mathrm{B}_S u_S(t) \\ y_S(t) &= \begin{bmatrix} 0 & -\frac{1680}{T_S^3} & 0 & -\frac{40}{T_S} \end{bmatrix} \mathbf{x}_S(t) + [1]\, u_S(t) \\ &= \mathrm{C}_S \mathbf{x}_S(t) + D_S u_S(t) \end{aligned} \quad \text{(II.2)}$$

where subscript S should be replaced by subscript CNS in the case of the central nervous system delay and subscript TL in the case of the torque loop dynamics. $\mathbf{x}_S(t)$ is the state space vector of the processing delay or torque control loop dynamics approximation.

$$\mathrm{A}_\mu = \begin{bmatrix} \begin{bmatrix} \mathrm{A}_{\mathrm{TL}} & 0 \\ 0 & \mathrm{A}_{\mathrm{CNS}} \end{bmatrix} & 0 & 0 \\ \begin{bmatrix} \mathrm{B}_A & 0 \\ 0 & \mathrm{B}_T \end{bmatrix} \begin{bmatrix} \mathrm{C}_{\mathrm{TL}} & 0 \\ 0 & \mathrm{C}_{\mathrm{CNS}} \end{bmatrix} & \begin{bmatrix} \mathrm{A}_A & 0 \\ 0 & \mathrm{A}_T \end{bmatrix} & 0 \\ \mathrm{B}_P \begin{bmatrix} \mathrm{D}_A & 0 \\ 0 & \mathrm{D}_T \end{bmatrix} \begin{bmatrix} \mathrm{C}_{\mathrm{TL}} & 0 \\ 0 & \mathrm{C}_{\mathrm{CNS}} \end{bmatrix} & \mathrm{B}_P \begin{bmatrix} \mathrm{C}_A & 0 \\ 0 & \mathrm{C}_T \end{bmatrix} & \mathrm{A}_P \end{bmatrix} \tag{II.8}$$

$$\mathrm{B}_\mu = \begin{bmatrix} \begin{bmatrix} \mathrm{B}_{\mathrm{TL}} & 0 \\ 0 & \mathrm{B}_{\mathrm{CNS}} \end{bmatrix} \\ \begin{bmatrix} \mathrm{B}_A & 0 \\ 0 & \mathrm{B}_T \end{bmatrix} \begin{bmatrix} \mathrm{D}_{\mathrm{TL}} & 0 \\ 0 & \mathrm{D}_{\mathrm{CNS}} \end{bmatrix} \\ \mathrm{B}_P \begin{bmatrix} \mathrm{D}_A & 0 \\ 0 & \mathrm{D}_T \end{bmatrix} \begin{bmatrix} \mathrm{D}_{\mathrm{TL}} & 0 \\ 0 & \mathrm{D}_{\mathrm{CNS}} \end{bmatrix} \end{bmatrix} \tag{II.9}$$

$$\mathrm{C}_\mu = \begin{bmatrix} [\mathrm{D}_A \mathrm{C}_{\mathrm{TL}} \quad 0] & [\mathrm{C}_A \quad 0] & 0 \\ \mathrm{D}_P \begin{bmatrix} \mathrm{D}_A & 0 \\ 0 & \mathrm{D}_T \end{bmatrix} \begin{bmatrix} \mathrm{C}_{\mathrm{TL}} & 0 \\ 0 & \mathrm{C}_{\mathrm{CNS}} \end{bmatrix} & \mathrm{D}_P \begin{bmatrix} \mathrm{C}_A & 0 \\ 0 & \mathrm{C}_T \end{bmatrix} & \mathrm{C}_P \end{bmatrix} \tag{II.10}$$

$$\mathrm{D}_\mu = \begin{bmatrix} [\mathrm{D}_A \mathrm{D}_{\mathrm{TL}} \quad 0] \\ \mathrm{D}_P \begin{bmatrix} \mathrm{D}_A & 0 \\ 0 & \mathrm{D}_T \end{bmatrix} \begin{bmatrix} \mathrm{D}_{\mathrm{TL}} & 0 \\ 0 & \mathrm{D}_{\mathrm{CNS}} \end{bmatrix} \end{bmatrix} \tag{II.11}$$

Equations $G_T(s) = 1/(sT_T + 1)$ and $G_A(s) = 1/(sT_A + 1)$ were rewritten in matrix form as

$$\begin{aligned} \dot{\mathbf{x}}_T(t) &= \left[-\frac{1}{T_T}\right] \mathbf{x}_T(t) + [1]\, y_{\mathrm{CNS}}(t) \\ &= \mathrm{A}_T \mathbf{x}_T(t) + \mathrm{B}_T y_{\mathrm{CNS}}(t) \\ \tau_2(t) &= \left[\frac{1}{T_T}\right] \mathbf{x}_T(t) + [0]\, y_{\mathrm{CNS}}(t) \\ &= \mathrm{C}_T \mathbf{x}_T(t) + D_T y_{\mathrm{CNS}}(t) \end{aligned} \tag{II.3}$$

and

$$\begin{aligned} \dot{\mathbf{x}}_A(t) &= \left[-\frac{1}{T_A}\right] \mathbf{x}_A(t) + [1] y_{\mathrm{TL}}(t) \\ &= \mathrm{A}_A \mathbf{x}_A(t) + \mathrm{B}_A y_{\mathrm{TL}}(t) \\ \tau_1(t) &= \left[\frac{1}{T_A}\right] \mathbf{x}_A(t) + [0] y_{\mathrm{TL}}(t) \\ &= \mathrm{C}_A \mathbf{x}_A(t) + D_A y_{\mathrm{TL}}(t) \end{aligned} \tag{II.4}$$

where $\mathbf{x}_T(t)$ and $\mathbf{x}_A(t)$ are state space vectors of trunk and ankle muscle activation dynamic models, respectively.

The stance dynamics model (10) vectors were defined as

$$\mathbf{x}_\mu(t) = \begin{bmatrix} \begin{bmatrix} \mathbf{x}_{\mathrm{TL}}(t) \\ \mathbf{x}_{\mathrm{CNS}}(t) \end{bmatrix} \\ \begin{bmatrix} \mathbf{x}_A(t) \\ \mathbf{x}_T(t) \end{bmatrix} \\ \mathbf{q}(t) \end{bmatrix} \tag{II.5}$$

where $\mathbf{x}_\mu(t)$ indicates the plant state vector that combines states of torque control loop dynamics $\mathbf{x}_{\mathrm{TL}}(t)$, CNS processing delay $\mathbf{x}_{\mathrm{CNS}}(t)$, activation dynamics of ankle $\mathbf{x}_A(t)$, trunk muscles $\mathbf{x}_T(t)$, and angles and angular velocities of double inverted pendulum structure $\mathbf{q}(t)$

$$\mathbf{u}_\mu(t) = [\, u_{\mathrm{TL}}(t) \quad u_{\mathrm{CNS}}(t)\,]^T \tag{II.6}$$

where the plant input vector $\mathbf{u}_\mu(t)$ consists of ankle $u_{\mathrm{TL}}(t)$ and trunk $u_{\mathrm{CNS}}(t)$ torque reference signals, and

$$\boldsymbol{\mu}(t) = [\, \tau_1(t) \quad \mathbf{q}^T(t)\,]^T \tag{II.7}$$

where plant output vector $\boldsymbol{\mu}(t)$ includes all directly measured system variables, namely, ankle torque $\tau_1(t)$, as well as angles and angular velocities of double inverted pendulum structure $\mathbf{q}(t)$.

The stance dynamics model (10) matrices were defined as shown in (II.8)–(II.11) at the top of the page, where A_μ is the system matrix, B_μ is the input matrix, C_μ is the output matrix, and D_μ is the input–output matrix.

Appendix III
Cost Function Weighting Matrices

The cost function (19) weighting matrices were defined as

$$\mathrm{R}_{\mathbf{xx}} = \left(\mathbf{U}_\mu^T + \mathbf{V}_\mu^T \mathrm{A}_\mu\right)^T \left(\mathbf{U}_\mu^T + \mathbf{V}_\mu^T \mathrm{A}_\mu\right) \tag{III.1}$$

$$\mathrm{R}_{\mathbf{xu}} = \left(\mathbf{U}_\mu^T + \mathbf{V}_\mu^T \mathrm{A}_\mu\right)^T \left(\mathbf{V}_\mu^T \mathrm{B}_\mu\right) \tag{III.2}$$

$$\mathrm{R}_{\mathbf{uu}} = \left(\mathbf{V}_\mu^T \mathrm{B}_\mu\right)^T \left(\mathbf{V}_\mu^T \mathrm{B}_\mu\right) + \mathrm{R}. \tag{III.3}$$

Acknowledgment

The authors would like to thank the impaired participants in this study, the physiotherapists P. Obreza and H. Benko for their assistance during measurements, and M. Ponikvar for the stimulator and the Matlab/Simulink interface design.

References

[1] A. Kralj and T. Bajd, *Functional Electrical Stimulation: Standing and Walking After Spinal Cord Injury*. Boca Raton, FL: CRC Press, 1989.

[2] T. Bajd, M. Munih, and A. Kralj, "Problems associated with FES-standing in paraplegia," *Technol. Health Care*, vol. 7, pp. 301–308, 1999.

[3] P. H. Veltink and N. Donaldson, "A perspective on the control of FES-supported standing," *IEEE Trans. Rehab. Eng.*, vol. 6, pp. 109–112, June 1998.
[4] K. Barin, "Evaluation of a generalized model of human postural dynamics and control in the sagittal plane," *Biol. Cyber.*, vol. 61, pp. 37–50, 1989.
[5] Z. Matjačić and T. Bajd, "Arm-free paraplegic standing—Part II: Experimental results," *IEEE Trans. Rehab. Eng.*, vol. 6, pp. 139–150, June 1998.
[6] K. J. Hunt and T. A. Johansen, "Design and analysis of gain-scheduled control using local controller networks," *Int. J. Contr.*, vol. 66, pp. 619–651, 1997.
[7] M. Munih, N. Donaldson, K. J. Hunt, and F. M. D. Barr, "Feedback control of unsupported standing in paraplegia. Part II: Experimental results," *IEEE Trans. Rehab. Eng.*, vol. 5, pp. 341–352, Dec. 1997.
[8] Z. Matjačić and T. Bajd, "Arm-free paraplegic standing—Part I: Control model synthesis and simulation," *IEEE Trans. Rehab. Eng.*, vol. 6, pp. 125–138, June 1998.
[9] L. M. Nashner and G. McCollum, "The organization of human postural movements: A formal basis and experimental synthesis," *Behav. Brain Sci.*, vol. 8, pp. 135–172, 1985.
[10] F. B. Horak and S. P. Moore, "The effect of prior leaning on human postural responses," *Gait Posture*, vol. 1, pp. 203–210, 1993.
[11] T. Sinha and B. E. Maki, "Effect of forward lean on postural ankle dynamics," *IEEE Trans. Rehab. Eng.*, vol. 4, pp. 348–359, Dec. 1996.
[12] P. C. Camana, H. Hemami, and C. W. Stockwell, "Determination of feedback for human posture control without physical intervention," *J. Cybern.*, vol. 7, pp. 199–225, 1977.
[13] H. Hemami, F. C. Weimer, C. S. Robinson, C. W. Stockwell, and V. S. Cvetkovic, "Biped stability considerations with vestibular models," *IEEE Trans. Automat. Contr.*, vol. AC-23, pp. 1074–1079, 1978.
[14] H. Hemami and A. Katbab, "Constrained inverted pendulum model for evaluating upright postural stability," *J. Dyn. Syst. Meas. Cont.*, vol. 104, pp. 343–349, 1982.
[15] A. D. Kuo, "An optimal control model for analyzing human postural balance," *IEEE Trans. Biomed. Eng.*, vol. 42, pp. 87–101, Jan. 1995.
[16] M. Mihelj, M. Munih, and M. Ponikvar, "Robust strategy for ankle joint torque control," in *Proc. 6th Annu. Conf. Int. Functional Electrical Stimulation Soc.*, Cleveland, OH, 2001, pp. 68–70.
[17] A. D. Kuo and F. E. Zajac, "A biomechanical analysis of muscle strength as a limiting factor in standing posture," *J. Biomech.*, vol. 26, pp. 137–150, 1993.
[18] L. Lublin and M. Athans, *The Control Handbook*, W. S. Levine, Ed. Boca Raton, FL: CRC/IEEE Press, 1996, ch. Linear quadratic regulator control, pp. 635–650.
[19] J. B. Burl, *Linear Optimal Control*. Reading, MA: Addison-Wesley Longman, 1998.
[20] M. Mihelj, Z. Matjačić, and T. Bajd, "Postural activity of constrained subject in response to disturbance in sagittal plane," *Gait Posture*, vol. 12, pp. 94–104, 2000.
[21] D. A. Winter, "Human balance and posture control during standing and walking," *Gait Posture*, vol. 3, pp. 193–214, 1995.
[22] R. J. Jaeger, "Design and simulation of closed-loop electrical stimulation orthoses for restoration of quiet standing in paraplegia," *J. Biomech.*, vol. 19, pp. 825–835, 1986.
[23] R.-P. Jaime, Z. Matjačić, and K. J. Hunt, "Paraplegic standing supported by FES-controlled ankle stiffness," *IEEE Trans. Neural Syst. Rehab. Eng.*, pp. 239–248, Dec. 2002.
[24] Z. Matjačić, M. Voigt, D. Popović, and T. Sinkjaer, "Functional postural responses after perturbations in multiple directions in a standing man: A principle of decoupled control," *J. Biomech.*, vol. 34, pp. 187–196, 2001.
[25] R. R. Riso, A. R. Ignagni, and M. W. Keith, "Cognitive feedback for use with FES upper extremity neuroprostheses," *IEEE Trans. Biomed. Eng.*, vol. 38, pp. 29–38, Jan. 1991.
[26] J. T. Gillis, *The Control Handbook*, W. S. Levine, Ed. Boca Raton, FL: CRC/IEEE Press, 1996, ch. State space, pp. 72–84.

Matjaž Mihelj received the B.Sc., M.Sc., and D.Sc. degrees from the Faculty of Electrical Engineering, University of Ljubljana, Slovenia, in 1996, 1999, and 2002, respectively.

Since 2003, he has been an Assistant Professor with the Faculty of Electrical Engineering, University of Ljubljana. He works in the fields of biomedical engineering and robotics. His current research interests are in man/machine interaction as well as modeling and control of biological systems with the main focus on restoration of lost functions in people with disabilities.

Dr. Mihelj is a member of IFMBE and IFESS. He received the Bedjani award from the Slovenian Ministry of Science and Technology and ISKRA Holding.

Marko Munih (M'88) received the B.Sc., M.Sc., and D.Sc. degrees in electrical engineering from the University of Ljubljana, Slovenia, in 1986, 1989, and 1993, respectively.

He is an Associate Professor and Head of the Laboratory of Robotics and Biomedical Engineering at the Faculty of Electrical Engineering, University of Ljubljana. His past research was focused on functional electrical stimulation of paraplegic lower extremities with surface electrode systems, including measurements, control, biomechanics, and electrical circuits. His interest is now focused on robot contact with environment and use of haptic interfaces in the field of rehabilitation engineering.

Dr. Munih is a member of IFMBE, IFESS, and IFAC. He received the Zois award in 2002 for outstanding scientific contrbutions from the Slovene Ministry of Science, Education and Sport.